Science
AAAS

# A Global Protein Kinase and Phosphatase Interaction Network in Yeast

Ashton Breitkreutz, *et al.*

*Science* **328**, 1043 (2010);
DOI: 10.1126/science.1176495

*This copy is for your personal, non-commercial use only.*

**If you wish to distribute this article to others**, you can order high-quality copies for your colleagues, clients, or customers by clicking here.

**Permission to republish or repurpose articles or portions of articles** can be obtained by following the guidelines here.

***The following resources related to this article are available online at www.sciencemag.org (this information is current as of May 31, 2010 ):***

**Updated information and services,** including high-resolution figures, can be found in the online version of this article at:
http://www.sciencemag.org/cgi/content/full/328/5981/1043

**Supporting Online Material** can be found at:
http://www.sciencemag.org/cgi/content/full/328/5981/1043/DC1

A list of selected additional articles on the Science Web sites **related to this article** can be found at:
http://www.sciencemag.org/cgi/content/full/328/5981/1043#related-content

This article **cites 22 articles**, 7 of which can be accessed for free:
http://www.sciencemag.org/cgi/content/full/328/5981/1043#otherarticles

This article has been **cited by** 1 articles hosted by HighWire Press; see:
http://www.sciencemag.org/cgi/content/full/328/5981/1043#otherarticles

This article appears in the following **subject collections**:
Cell Biology
http://www.sciencemag.org/cgi/collection/cell_biol

Downloaded from www.sciencemag.org on May 31, 2010

*Science* (print ISSN 0036-8075; online ISSN 1095-9203) is published weekly, except the last week in December, by the American Association for the Advancement of Science, 1200 New York Avenue NW, Washington, DC 20005. Copyright 2010 by the American Association for the Advancement of Science; all rights reserved. The title *Science* is a registered trademark of AAAS.

at pH 5.0. This complex is likely to interact with the cytoplasmic region of basal body of the secretion apparatus and to respond to an unidentified pH sensor. The sensor is unlikely to be part of the translocon because the translocon deletion mutant displayed wild-type levels of effector secretion upon pH upshift (fig. S7). The sensor might be the needle subunit itself, which has been implicated in signaling the translocator to effector switch in *Shigella* (*11*) and Yop secretion by *Yersinia* (*12*). Another possibility is that translocon pore assembly changes the pH gradient within the needle channel and that the sensor is located toward the base of the secretion apparatus. Changes in pH from mildly acidic to neutral can have dramatic effects on protein folding; for example, some bacterial toxins refold after their translocation from acidic endosomes to the host-cell cytosol in a partially unfolded state (*13*). The SPI-2 T3SS pH sensor might thus undergo a conformational change on exposure to neutral pH and transduce a dissociation signal to the SsaL/SsaM/SpiC complex.

### References and Notes


1. J. E. Galán, H. Wolf-Watz, *Nature* **444**, 567 (2006).
2. C. Rappl, J. Deiwick, M. Hensel, *FEMS Microbiol. Lett.* **226**, 363 (2003).
3. D. Chakravortty, M. Rohde, L. Jäger, J. Deiwick, M. Hensel, *EMBO J.* **24**, 2043 (2005).
4. X.-J. Yu, M. Liu, D. W. Holden, *Mol. Microbiol.* **54**, 604 (2004).
5. M. J. Pallen, S. A. Beatson, C. M. Bailey, *BMC Microbiol.* **5**, 9 (2005).
6. B. K. Coombes, N. F. Brown, Y. Valdez, J. H. Brumell, B. B. Finlay, *J. Biol. Chem.* **279**, 49804 (2004).
7. Materials and methods are available as supporting material on *Science* Online.
8. F. D. Schubot *et al.*, *J. Mol. Biol.* **346**, 1147 (2005).
9. D. Drecktrah, L. A. Knodler, D. Howe, O. Steele-Mortimer, *Traffic* **8**, 212 (2007).
10. C. R. Beuzón, G. Banks, J. Deiwick, M. Hensel, D. W. Holden, *Mol. Microbiol.* **33**, 806 (1999).
11. R. Kenjale *et al.*, *J. Biol. Chem.* **280**, 42929 (2005).
12. J. Torruellas, M. W. Jackson, J. W. Pennock, G. V. Plano, *Mol. Microbiol.* **57**, 1719 (2005).
13. J. A. Young, R. J. Collier, *Annu. Rev. Biochem.* **76**, 243 (2007).



14. We thank J. Mota, C. Tang, and members of the Holden laboratory for comments on the manuscript. This research was supported by grants G0800148 and 074553/Z/04/Z to D.W.H. from the Medical Research Council and Wellcome Trust.


### Supporting Online Material

www.sciencemag.org/cgi/content.full/science.1189000/DC1
Materials and Methods
Figs. S1 to S8
References


2 March 2010; accepted 25 March 2010
Published online 15 April 2010;
10.1126/science.1189000
Include this information when citing this paper.


Downloaded from www.sciencemag.org on May 31, 2010

# A Global Protein Kinase and Phosphatase Interaction Network in Yeast


**Ashton Breitkreutz,[1]* Hyungwon Choi,[2]* Jeffrey R. Sharom,[1,3]* Lorrie Boucher,[1]* Victor Neduva,[4]* Brett Larsen,[1] Zhen-Yuan Lin,[1] Bobby-Joe Breitkreutz,[1] Chris Stark,[1] Guomin Liu,[1] Jessica Ahn,[1] Danielle Dewar-Darch,[1] Teresa Reguly,[1] Xiaojing Tang,[1] Ricardo Almeida,[4] Zhaohui Steve Qin,[5] Tony Pawson,[1,3] Anne-Claude Gingras,[1,3]† Alexey I. Nesvizhskii,[2,6]† Mike Tyers[1,3,4]†**



The interactions of protein kinases and phosphatases with their regulatory subunits and substrates underpin cellular regulation. We identified a kinase and phosphatase interaction (KPI) network of 1844 interactions in budding yeast by mass spectrometric analysis of protein complexes. The KPI network contained many dense local regions of interactions that suggested new functions. Notably, the cell cycle phosphatase Cdc14 associated with multiple kinases that revealed roles for Cdc14 in mitogen-activated protein kinase signaling, the DNA damage response, and metabolism, whereas interactions of the target of rapamycin complex 1 (TORC1) uncovered new effector kinases in nitrogen and carbon metabolism. An extensive backbone of kinase-kinase interactions cross-connects the proteome and may serve to coordinate diverse cellular responses.


Protein phosphorylation mediates cellular responses to growth factors, environmental signals, and internal processes by the regulation of protein interactions, enzyme activity, or protein localization (*1*). However, the protein interactions of kinases, phosphatases, and their regulatory subunits and substrates remain sparsely mapped, particularly in high-throughput (HTP) datasets [fig. S1 (*2*)]. To chart the budding yeast kinase and phosphatase interaction (KPI) network, we systematically characterized protein kinase and phosphatase complexes by rapid magnetic bead capture, on-bead protein digestion, and mass spectrometric identification of associated proteins, using different epitope tags and expression systems [fig. S2; (*2*)]. One hundred thirty protein kinases, 24 lipid and metabolic kinases, 47 kinase regulatory subunits, 38 protein phosphatases, 32 phosphatase regulatory subunits, and 5 metabolic phosphatases were analyzed (tables S1 and S2).

We eliminated nonspecific interactions using a statistical model called Significance Analysis of Interactome (SAINT). In contrast to simple threshold models, SAINT assigns the number of peptide identifications for each interactor to a probability distribution, which is then used to estimate the likelihood of a true interaction (*2*). We validated SAINT on multiple independent purifications for several kinases and expression levels (fig. S3 and tables S3 to S5). A final KPI dataset of 1844 interactions between 887 protein partners was generated from more than 38,000 unfiltered identifications at a stringent SAINT threshold of $P > 0.85$ (fig. S4 and tables S1 and S2). High-confidence interactions were recovered for 120 protein kinases (fig. S5; see fig. S6 and table S6 for validation). For a number of kinases, we demonstrated that associated proteins were substrates in vitro (figs. S7 and S8 and table S7). Our dataset doubled the number of KPIs obtained in previous low-throughput (LTP) studies and performed as well as LTP data against an unbiased HTP high-confidence (HTP-HC) benchmark dataset [fig. S1 (*2*)]. Clustering of all kinases and phosphatases by their interaction profiles revealed locally dense regions in the KPI network (Fig. 1A and fig. S9).

The Cdc14 phosphatase formed one of the largest single hubs in the network with 53 interaction partners, including 23 kinases and 5 phosphatases (Fig. 1B, fig. S6, and table S6). Cdc14 antagonizes mitotic cyclin-dependent kinase (CDK) activity and is activated by the mitotic exit network (MEN) upon completion of anaphase (*3*). Many Cdc14 interactors were shared with its anchor protein Net1 and the nicotinamide adenine dinucleotide ($NAD^+$)–dependent histone deacetylase Sir2 that together with Cdc14 form the nucleolar RENT complex (*4*). New connections between Cdc14 and other mitotic regulators included the CDK-inhibitory kinase Swe1, the cytokinesis checkpoint protein Boi1 (*5*), and two activators of cytokinesis, Cbk1 and Ace2 (*6*). Cdc14, Net1, and Sir2 each interacted with the DNA damage checkpoint kinases Chk1 and Dun1. In support of a role for Cdc14 in the DNA damage response, we found that ectopic expression of Cdc14 caused sensitivity to the DNA-damaging agent methylmethane sulfonate (MMS), while a strain defective for Cdc14 function was sensitive to the ribonucleotide reductase inhibitor hydroxyurea (Fig. 1C). Interactions between the


[1]Centre for Systems Biology, Samuel Lunenfeld Research Institute, 600 University Avenue, Toronto, Ontario, M5G 1X5, Canada. [2]Department of Pathology, University of Michigan, Ann Arbor, MI 48109, USA. [3]Department of Molecular Genetics, University of Toronto, 1 Kings College Circle, Toronto, Ontario, M5S 1A8, Canada. [4]Wellcome Trust Centre for Cell Biology and School of Biological Sciences, University of Edinburgh, Mayfield Road, Edinburgh, EH9 3JR Scotland, UK. [5]Department of Biostatistics, University of Michigan, Ann Arbor, MI 48109, USA. [6]Center for Computational Medicine and Bioinformatics, University of Michigan, Ann Arbor, MI 48109, USA.

*These authors contributed equally to this work.
†To whom correspondence should be addressed. E-mail: gingras@lunenfeld.ca (A.C.G.), nesvi@med.umich.edu (A.I.N.), tyers@lunenfeld.ca, m.tyers@ed.ac.uk (M.T.)

RENT and the nutrient-sensing TOR complex 1 (TORC1) were supported by the finding that increased Cdc14 activity caused rapamycin sensitivity, whereas reduced Cdc14 function caused rapamycin resistance (Fig. 1D), suggesting that Cdc14 may antagonize TOR signaling. Cdc14 also interacted with the energy-sensing adenosine 5′-monophosphate (AMP)–activated kinase (AMPK) Snf1 and its upstream kinase Sak1; AMPK activates glucose-repressed genes in yeast and is an upstream inhibitor of TOR activity in metazoans (*7*). Deregulation of Cdc14 caused a severe defect in growth on glycerol medium and sensitivity to 2-deoxyglucose (Fig. 1D).

Cdc14 exhibited connections with three different mitogen-activated protein kinase (MAPK) modules. Interaction of the pheromone MAPK pathway kinases Fus3 and Ste7 with Cdc14 was supported by the finding that constitutive expression of Cdc14 caused partial pheromone resistance (fig. S10). Cdc14 interacted with the high osmolarity glycerol (HOG) pathway MAPK kinase Pbs2; consistently, constitutive expression of Cdc14 caused sensitivity to osmotic stress (Fig. 1E). The HOG pathway is also known to stimulate mitotic exit (*8*). The upstream cell wall integrity (CWI) MAPK kinase Bck1 interacted with Cdc14; a *cdc14-3* strain was sensitive to the cell wall stress agent calcofluor white (Fig. 1E). These CWI interactions extended along each pathway because the conditional MEN alleles *mob1-77* and *cdc15-2* exhibited specific synthetic lethal interactions with either *slt2*Δ or *bck1*Δ mutations; this lethality was alleviated by growth on iso-osmotic medium but not by a catalytically inactive mutant of Slt2 (Fig. 1F and fig. S10). These data reveal Cdc14 as a nexus for cell cycle, checkpoint, metabolic, and stress signals (fig. S10).

The TORC1 and TORC2 kinase complexes are conserved from yeast to human and control macromolecular synthesis and polarized morphogenesis, respectively; TORC1 is sensitive to the macrolide rapamycin, whereas TORC2 is not (*9*). In the KPI dataset, TORC1 and TORC2 formed a highly connected subnetwork of 28 interaction partners, including 13 kinases and 4 phosphatases (figs. S6 and S11 and table S6). These connections established new links between TORC1 and the mitochondrial retrograde (RTG) signaling pathway (*10*), which induces genes required for glutamate production (fig. S12). Multiple TORC1 subunits exhibited previously undocumented interactions with the kinases Fmp48, Nnk1, Npr1, and Ksp1 (Fig. 2A and fig. S11).

Fmp48 is a kinase of unknown function that is associated with mitochondrial subcellular fractions (*11*). Consistent with interactions among

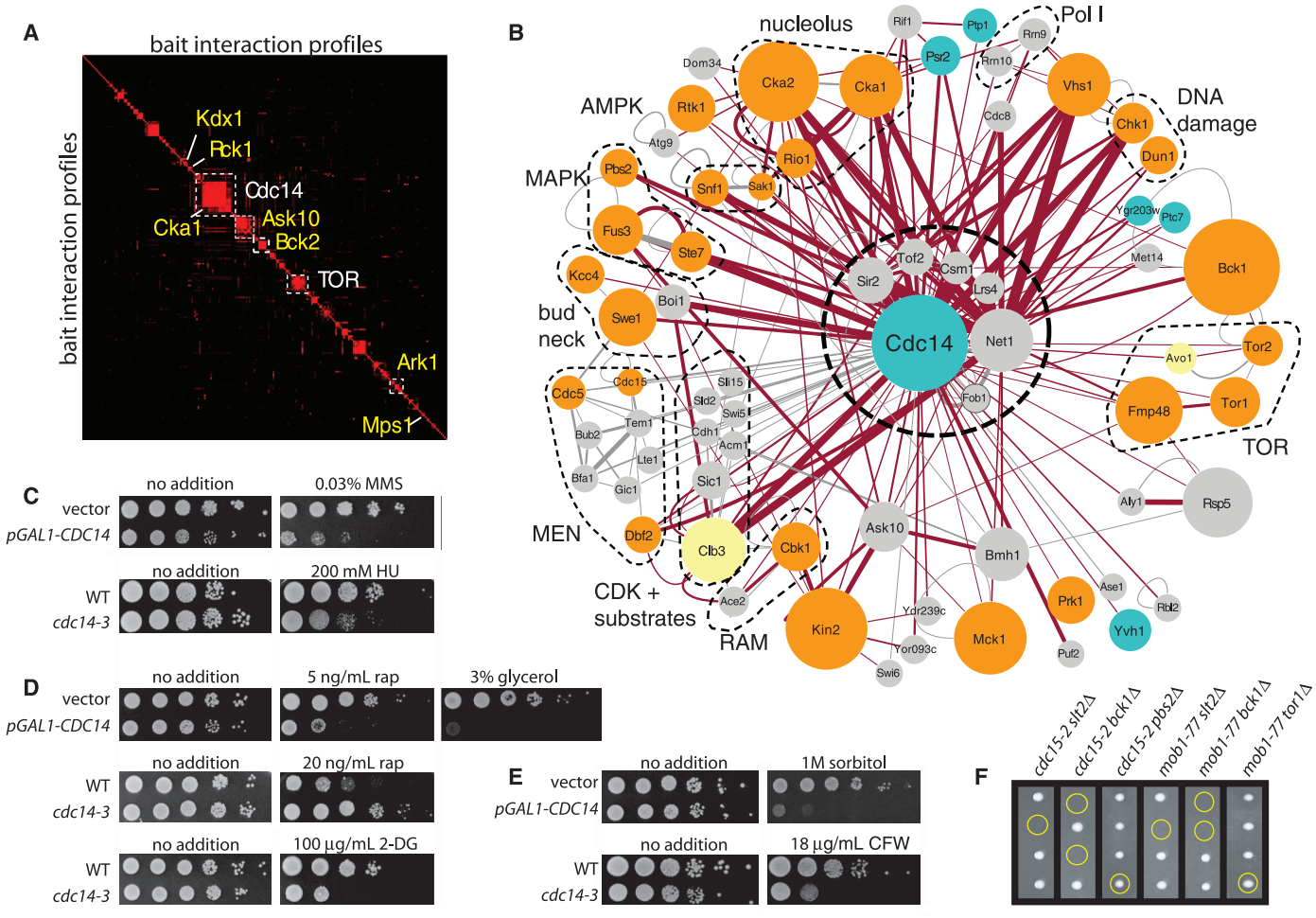


**Fig. 1.** Cdc14 phosphatase network. (**A**) Hierarchical two-dimensional clustering of bait interaction profiles in the KPI dataset. See fig. S9 for full clustergram. Networks for indicated clusters and other kinases are shown in fig. S19. (**B**) Cdc14-Net1-Sir2 (RENT) interaction network. Kinases are in orange, phosphatases in blue, kinase-associated proteins in yellow, and other proteins in gray. Red connecting lines indicate KPI interactions, gray lines LTP interactions, and gray dashed lines HTP-HC interactions. Line thickness indicates peptide count of interaction; node size is proportional to total number of interactions in the KPI dataset. Bold dashed circle indicates RENT complex and known associated proteins. RAM, regulation of Ace2p activity and cellular morphogenesis. (**C**) Sensitivity of a *GAL1-CDC14* strain to 0.03% methyl methanesulfonate (MMS) when induced by 0.02% galactose (see fig. S20 for expression titration) and a *cdc14-3* strain to 200 mM hydroxyurea (HU) at 33°C. (**D**) Sensitivity of a *GAL1-CDC14* strain to either rapamycin (5 ng/ml) or glycerol medium when induced by 0.05% galactose. Resistance of a *cdc14-3* strain to rapamycin (20 ng/ml) and sensitivity to 2-deoxyglucose (DG, 100 µg/ml) at 33°C. (**E**) Sensitivity of a *GAL1-CDC14* strain to 1 M sorbitol when induced by 0.05% galactose. Sensitivity of a *cdc14-3* strain to calcofluor white (CFW, 18 µg/ml) at 33°C. (**F**) Representative tetrads bearing combinations of *slt2*Δ, *bck1*Δ, *cdc15-2*, and *mob1-77* alleles. Double-mutant spore clones are circled in yellow; *pbs2*Δ and *tor1*Δ served as negative controls.

Downloaded from www.sciencemag.org on May 31, 2010

Fmp48, TORC1, and the RTG inhibitor Mks1, elevated expression of *FMP48* caused a growth defect on nonfermentable glycerol medium and rapamycin resistance on a fermentable carbon source (Fig. 2B). Overexpression of *FMP48* caused abnormal mitochondrial morphology (Fig. 2C) and repression of genes encoding tricarboxylic acid cycle enzymes, electron transport chain components, and subunits of the adenosine 5′-triphosphate (ATP) synthase (Fig. 2D). Fmp48-associated kinase activity was specifically increased by rapamycin treatment (Fig. 2E), suggesting that Fmp48 relays TORC1 signals to the RTG pathway and mitochondrial function.

The uncharacterized kinase Ykl171w, renamed Nnk1 for nitrogen network kinase, associated with all TORC1 subunits (fig. S11) and with Gdh2, the $NAD^+$-dependent glutamate dehydrogenase that catalyzes deamination of glutamate to α-ketoglutarate and ammonia (*12*). Gdh2 was phosphorylated by Nnk1 complexes in vitro (Fig. 2F), and a *gdh2*Δ strain was resistant to rapamycin when grown on glutamate as the sole nitrogen source (Fig. 2G), whereas overexpression of *NNK1* conferred hypersensitivity to rapamycin (Fig. 2H). Nnk1 also interacted with the TORC1 effector Ure2, which regulates the nitrogen catabolite response by sequestering the transcription factor Gln3 in the cytoplasm (*12*). Overexpression of *NNK1* induced rapid nuclear accumulation of Gln3 (Fig. 2I) and increased transcription of Gln3 target genes (Fig. 2J), suggesting that Nnk1 activity antagonizes the Ure2-Gln3 inter-

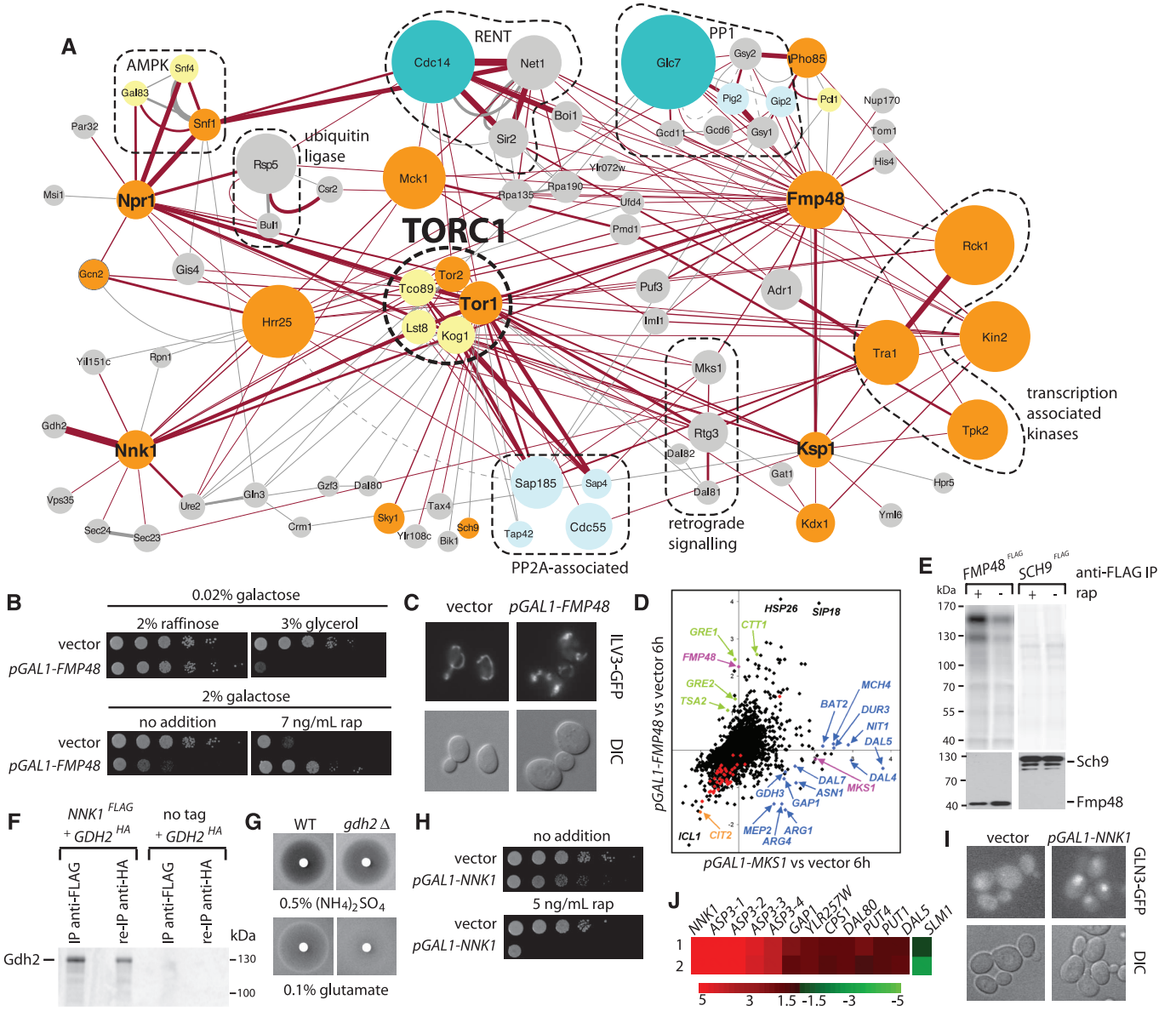


**Fig. 2.** TORC1 kinase network. (**A**) Partial network of new TORC1-associated kinases. (**B**) Overexpression of *GAL1-FMP48* inhibits growth on glycerol and confers rapamycin resistance. (**C**) Overexpression of *GAL1-FMP48* causes abnormal mitochondrial morphology as visualized with an $Ilv3^{GFP}$ mitochondrial matrix fusion protein (GFP, green fluorescent protein). DIC, differential interference contrast. (**D**) Genome-wide expression profiles of *GAL1-FMP48* and *GAL1-MKS1* strains induced with 0.2% galactose. RTG-responsive (orange), mitochondrial (red), stress-responsive (green), and Gln3/Gcn4-responsive (blue) genes are marked. (**E**) $Fmp48^{FLAG}$ or $Sch9^{FLAG}$ complexes were immunopurified from cells grown in the presence or absence of rapamycin (200 ng/ml) for 30 min, then incubated with $[^{33}P]$-γ-ATP, and radiolabeled species were resolved by SDS–polyacrylamide gel electrophoresis. Nonregulated Sch9-associated activity served as a negative control. (**F**) Immunopurified $Nnk1^{FLAG}$ complexes were incubated with $[^{33}P]$-γ-ATP, then denatured, and radiolabeled Gdh2 species were repurified with antibody to hemagglutinin (HA). (**G**) A *gdh2Δ* strain is rapamycin resistant when glutamate is the sole nitrogen source. (**H**) Expression of *GAL1-NNK1* in 2% galactose confers sensitivity to rapamycin (5 ng/ml). (**I**) Expression of *GAL1-NNK1* in 2% galactose for 1 hour causes nuclear accumulation of $Gln3^{GFP}$. (**J**) Expression of *GAL1-NNK1* in 0.2% galactose for 1.5 hours specifically induces Gln3 target genes. Color bar indicates fold increase (red) or decrease (green) relative to empty vector control.

Downloaded from www.sciencemag.org on May 31, 2010

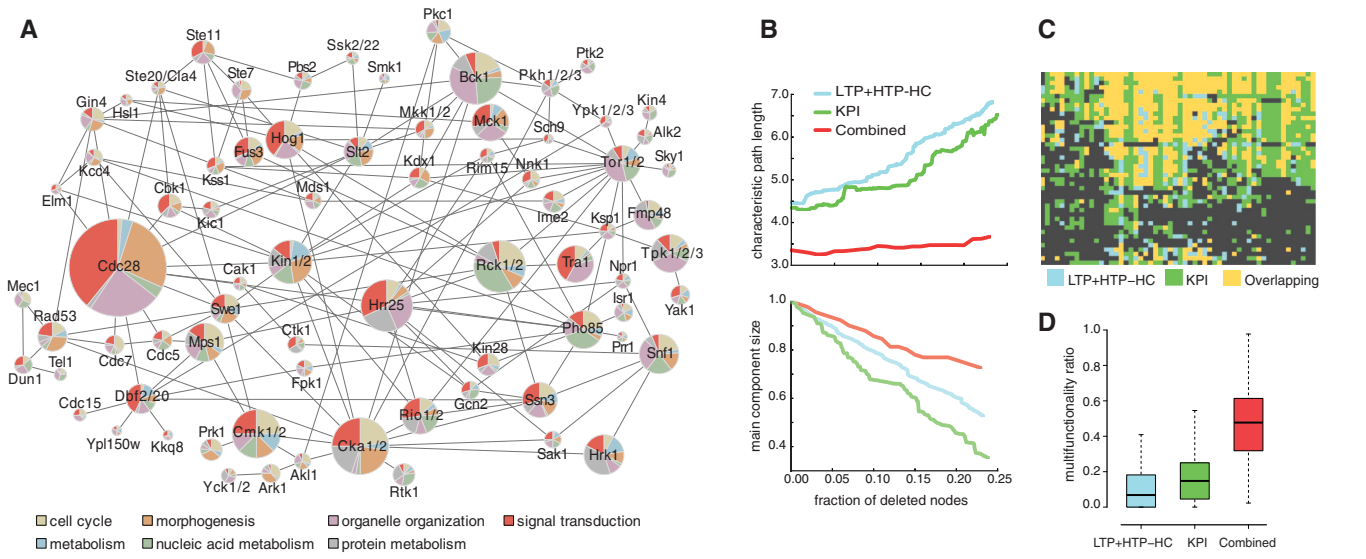


**Fig. 3.** A kinase-kinase (K-K) network connects the proteome. (**A**) Combined K-K interaction network derived from the KPI, LTP, and HTP-HC datasets. Interactions from known kinase regulatory subunits and paralogs were collapsed into single nodes (table S8). The reduced network contains 156 interactions between 75 kinases, 66 of which contain documented phosphorylation sites (table S9). Colors indicate fraction of GO Super-Slim biological processes assigned by interaction partners of each kinase (*2*). (**B**) Nodes in the combined K-K network were deleted in decreasing degree order. Characteristic path length and largest residual connected component were normalized to initial values. K-K networks derived from KPI and LTP+HTP-HC datasets were used as controls. (**C**) Clustering of GO Slim biological processes associated with kinase interaction partners. Full clustergram is shown in fig. S17. (**D**) Multifunctionality of kinase associations. Ratio indicates number of GO Slim biological processes per kinase normalized to all processes (*2*).

action. The expansive TORC1 network also included other nutrient-sensing kinases (Npr1, Snf1, Gcn2, and Ksp1; fig. S11) (*13*), transcription-associated kinases (Tra1 and Tpk2), MAPK module components (Bck1 and Kdx1), cell cycle kinases (Ime2, Mih1, and Clb2-Cdc28), an mRNA splicing kinase (Sky1), and a ribosome biogenesis kinase (Rio2). These findings underscore the central role of TOR in cell growth.

In a global protein interaction network constructed from the KPI, LTP, and HTP-HC datasets (*2*), kinase-kinase (K-K) interactions were significantly enriched compared to all other kinase interaction partners ($P < 3 \times 10^{-6}$) and collectively formed a highly interconnected K-K network (Fig. 3A, figs. S13 and S14, and table S8). Consistent with a trans-kinase phosphorylation network (*14*), we assigned 607 phosphorylation sites on 98 kinases (fig. S15 and table S9). This K-K network was extremely robust to fragmentation by hub deletion (Fig. 3B) and was far less modular than previous less-complete K-K networks [fig. S16 (*2*)]. Within the global network, kinases had a significantly higher centrality compared to nonkinase nodes [$P < 10^{-16}$ (*2*)], suggesting that kinases might unify cellular regulation. To test this idea, we identified dense clusters of interactions (cliques or complexes) in the global interaction network, then determined the extent of clique cross-connection by kinase interactions. More than 80% of the proteome was interlinked by kinases in this manner (fig. S17), a significantly larger fraction than in random networks [$P < 10^{-8}$ (*2*)]. The potential for kinases to co-regulate otherwise separate functions was further revealed by the diversity of Gene Ontology (GO) biological processes associated with kinase interaction partners (Fig. 3C and fig. S18). The multifunctionality of kinases, as defined by associated GO terms, was markedly increased by the KPI dataset (Fig. 3D).

Cellular processes are controlled by a multitude of low-affinity interactions, as often mediated by short linear motifs embedded in disordered protein regions (*15*, *16*). The KPI network is highly enriched for disordered regions as compared to the entire proteome [$P < 10^{-16}$ (*2*)]. This physical organization may allow the cell to overcome stochastic limitations in signal propagation, integration, and downstream responses (*16*). In human cells, kinase-mediated signaling can readily propagate across pathways (*17*) and may dictate complex decisions through a broadly distributed network of effectors (*18*, *19*). Moreover, phosphorylation-based feedback loops often enable cooperative responses, tuning of network outputs, and entrained states (*20*–*22*). The densely connected and nonmodular architecture of the KPI network suggests that the interaction of many such circuits will underpin cellular information flow (*23*).

### References and Notes


1. T. Pawson, *Curr. Opin. Cell Biol.* **19**, 112 (2007).
2. Supporting material is available on *Science* Online.
3. F. Stegmeier, A. Amon, *Annu. Rev. Genet.* **38**, 203 (2004).
4. A. F. Straight *et al.*, *Cell* **97**, 245 (1999).
5. M. Mendoza *et al.*, *Nat. Cell Biol.* **11**, 477 (2009).
6. B. Nelson *et al.*, *Mol. Biol. Cell* **14**, 3782 (2003).
7. D. G. Hardie, *Nat. Rev. Mol. Cell Biol.* **8**, 774 (2007).
8. V. Reiser, K. E. D'Aquino, L. S. Ee, A. Amon, *Mol. Biol. Cell* **17**, 3136 (2006).
9. S. Wullschleger, R. Loewith, M. N. Hall, *Cell* **124**, 471 (2006).
10. Z. Liu, R. A. Butow, *Annu. Rev. Genet.* **40**, 159 (2006).
11. J. Reinders, R. P. Zahedi, N. Pfanner, C. Meisinger, A. Sickmann, *J. Proteome Res.* **5**, 1543 (2006).
12. B. Magasanik, *Proc. Natl. Acad. Sci. U.S.A.* **102**, 16537 (2005).
13. A. Huber *et al.*, *Genes Dev.* **23**, 1929 (2009).
14. A. Chi *et al.*, *Proc. Natl. Acad. Sci. U.S.A.* **104**, 2193 (2007).
15. V. Neduva *et al.*, *PLoS Biol.* **3**, e405 (2005).
16. T. J. Gibson, *Trends Biochem. Sci.* **34**, 471 (2009).
17. W. M. Old *et al.*, *Mol. Cell* **34**, 115 (2009).
18. H. Daub *et al.*, *Mol. Cell* **31**, 438 (2008).
19. A. von Kriegsheim *et al.*, *Nat. Cell Biol.* **11**, 1458 (2009).
20. J. E. Ferrell Jr., *Curr. Opin. Cell Biol.* **14**, 140 (2002).
21. F. Li, T. Long, Y. Lu, Q. Ouyang, C. Tang, *Proc. Natl. Acad. Sci. U.S.A.* **101**, 4781 (2004).
22. Q. A. Justman, Z. Serber, J. E. Ferrell Jr., H. El-Samad, K. M. Shokat, *Science* **324**, 509 (2009).
23. P. Nurse, *Nature* **454**, 424 (2008).


24. We thank B. Raught, A. Amon, L. Harrington, J. Bader, M. Costanzo, B. Andrews, C. Boone, R. Aebersold, B. Bodenmiller, I. Sadowski, and F. Sicheri for discussions; J. P. Zhang and D. Fermin for technical support; and M. Snyder, Y. Ohsumi, S. Piatti, S. Hahn, H. Reizman, S. Biggins, T. Petes, M. P. Longhese, and D. Mao for reagents. Supported by grants from the Canadian Institutes of Health Research to A.C.G. (MOP-84314), T.P. (MOP-57793), and M.T. (MOP-12246); the Ontario Research Fund to T.P. and A.C.G. (REO#-044); the National Institutes of Health to M.T. (R01RR024031 from the National Center for Research Resources) and A.I.N. (CA-126239); a Terry Fox Foundation Research Studentship from the National Cancer Institute of Canada to J.R.S.; Federation of European Biochemical Societies and Marie Curie Fellowships to V.N.; Canada Research Chairs in Functional Genomics and Bioinformatics (to M.T.) and in Functional Proteomics (to A.C.G.); the Lea Reichmann Chair in Cancer Proteomics to A.C.G.; and a Scottish Universities Life Sciences Alliance Research Professorship and a Royal Society Wolfson Research Merit Award to M.T.


### Supporting Online Material

www.sciencemag.org/cgi/content/full/328/5981/1043/DC1
Materials and Methods
Figs. S1 to S27
Tables S1 to S15
References

19 May 2009; accepted 7 April 2010
10.1126/science.1176495

Downloaded from www.sciencemag.org on May 31, 2010